

# Heat radiation reduction in the cryostat with multilayer insulation technique

---

**D. Singh,<sup>a,1</sup> A. Pandey,<sup>a,</sup> M. K. Singh,<sup>a,c</sup> L. Singh,<sup>b</sup> V. Singh,<sup>a,b,2</sup>**

<sup>a</sup>*Banaras Hindu University, Department of Physics, Institute of Science  
Varanasi-221005, India*

<sup>b</sup>*Central University of South Bihar, Physics Department, School of Physical and Chemical Sciences  
Gaya-824236, India*

<sup>c</sup>*Institute of Physics, Academia Sinica  
Taipei-11529, Taiwan*

*E-mail:* [daminisinghphy27@gmail.com](mailto:daminisinghphy27@gmail.com), [venkaz@yahoo.com](mailto:venkaz@yahoo.com)

**ABSTRACT:** Multilayer insulation (MLI) is an important technique for the reduction of radiation heat load in cryostats. The present work is focused on investigation for the selection of suitable reflective layer and spacer material in MLI systems. In our analysis, we have selected perforated double-Aluminized Mylar (DAM) with Dacron, unperforated DAM with Silk-net and perforated DAM with Glass-tissue for their evaluation as the reflective layer as well as spacer materials in MLI technique. Current work would discuss the calculation of the effect of layer density and the number of layers on the heat load. Knowing the key parameters of MLI, we have compared the heat load generation in spherical as well as cylindrical cryostats and the effect of layering near and outer surface on the heat load.

**KEYWORDS:** Cryostat; Heat load; Multilayer insulation

---

<sup>1</sup>Corresponding author.

<sup>2</sup>Corresponding author.

---

## Contents

<b>1</b>	<b>Introduction</b>	<b>1</b>
<b>2</b>	<b>Heat exchange between the two surfaces of a cryostat</b>	<b>3</b>
<b>3</b>	<b>Optimization of the layer density in MLI technique</b>	<b>6</b>
<b>4</b>	<b>Results and discussion</b>	<b>9</b>
4.1	MLI testing material	9
4.2	Analysis of the key parameters in MLI technique	10
4.2.1	Enhancement in layer density and its effect on the heat load	10
4.2.2	Selection of optimal layer density	12
4.2.3	Effects of increment in the number of layers over the heat load	13
4.3	Preference in the geometry of the cryostat	14
<b>5</b>	<b>Summary and conclusion</b>	<b>16</b>

---

## 1 Introduction

The word cryostat (also called as “dewars” in the memories of Sir James Dewar) is made up of two words cryo and stat, which means cold and stable [1]. Typically, it is a container filled with cryogenic liquid (Liquid Argon (LAr), Liquid Helium (LHe), Liquid Nitrogen (LN<sub>2</sub>), and Liquid Hydrogen (LH<sub>2</sub>) etc.) to provide mechanical housing, cooling and shielding against the residual environmental backgrounds to the device under consideration at very low temperature for its safe and stable operation [2]. Evidently, steady functioning requires minimum heat load (thermal radiation, solid conduction and gas conduction) near the inner wall of the cryostat. The requirement of minimum heat load (Particularly radiation heat load) can be well accomplished by using the multilayer insulation (MLI) technique. The basic principle of MLI technique is to obtain the multiple radiation reflection by placing the reflective layers called as radiation shields, in the vacuum space between the two walls (hot radiating surface and cold surface) of the cryostat [3]. These reflective layers are usually made up of thin polyethylene or Mylar sheet, coated with highly reflecting material (Aluminium or Gold, but most commonly Aluminium is used due to low cost) on both sides [4]. It follows that there may be a chance of conduction due to adjacent reflective layers. Therefore, low conductivity materials or insulators called as spacers are placed in between these reflective layers. As these reflective layers are interleaved with insulating spacers, they do not touch each other and minimize the thermal heat exchange/thermal conduction [5]. A schematic diagram of the MLI structure consists of reflective layers interleaved with insulating spacers is shown in figure 1.

Vigorous thermal insulation systems of MLI technique are required for developing the efficient storage and transfer of cryogenics [6]. It is a passive thermal protection system widely used in cryogenics and space exploration programs as an excellent thermal insulator [5]. MLI technique has extensive applications in storage, transfer, thermal protection, and low-temperature processes. The present work focuses on thermal protection and low-temperature applications of MLI technique in fundamental physics research experiments. MLI technique is being used worldwide in numerous basic physics research experiments such as: exploration of space (NASA [6, 7]), accelerators (LHC [2, 8]), dark matter searches (EDELWEISS [9, 10], CRESST [11, 12], EURECA [13]), and the searches of neutrinoless double  $\beta$ -decay (CUORE [14], GERDA [15, 16], and in future LEGEND [17]), etc. These broad fields of applications reveal the enthusiasm of the scientists working in this field worldwide. There are ample cryogenic thermal research works being performed after the first experimental test on MLI by Sir James Dewar in 1900 when he tested with three layers of Aluminum foil (current form of MLI with layered radiation shield system was described firstly by William D. Cornell in the late 1940s) [18, 19].

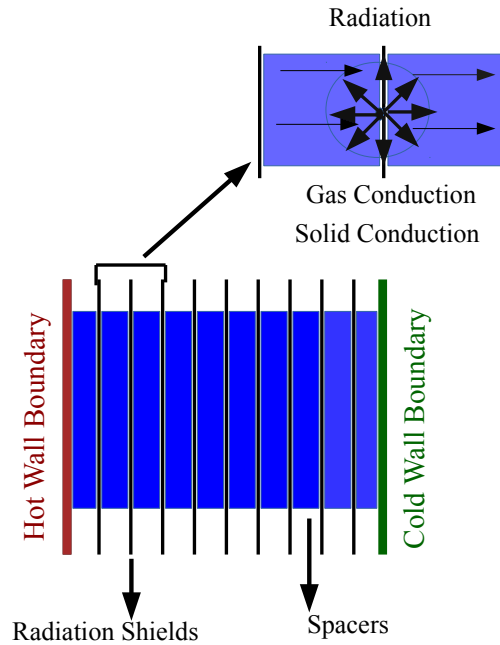


**Figure 1.** Schematic diagram of the MLI structure consists of reflective layers interleaved with insulating spacers. The heat exchange (via heat radiation, solid conduction and gas conduction) between two consecutive reflective layers is depicted in its inset.

The design, analysis, and testing of a given MLI system depend on the nature and requirements of the specific application. Generally, MLI systems are used in high vacuum environments, which may be a vacuum vessel or space such as the Earth's orbit or the lunar surface [7]. This is because MLI is the ideal insulation for the radiation dominated heat transfer environments such as spacecraft in the low Earth orbit and the other high vacuum functions [20]. Furthermore, MLI systems can also be designed for soft vacuum purposes in industrial products as well as in commercial building apparatus [21]. Nevertheless, MLI systems can also be constructed for no vacuum (at ambient pressure) applications where radiation heat transfer is a significant amount

of the total heat gain in moderate temperature (non–cryogenic) thermal protection systems [7]. Tremendously low temperature ( $\leq 4$  K) refrigeration is also attainable by MLI systems, which have numerous worldwide applications in basic physics research [5].

The current work is an attempt to address the question of what is the best MLI system, which is usually asked before designing the cryostat in an experiment. Although reducing the heat load in a system is the primary aim, it should not be too much costly as well as should not take too much time in operations. It follows that the correct methodology would be to proceed via an appropriate “thermo–economic” approach in achieving the best MLI system. In this direction, the selection of suitable material and appropriate design are very crucial. Furthermore, the level of vacuum (incorporating the level of vacuum between the layers also) and the layer density are even more pivotal for getting the better efficiency of the MLI system. The present work is focused on the selection of suitable material with optimum layer density to minimize the heat/thermal radiation (the most prominent contribution in the total thermal budget for cryostats) and achieve the best MLI system for the spherical and cylindrical cryostats.

## 2 Heat exchange between the two surfaces of a cryostat

Cryostats are made up of metals and due to environmental effects, there are always some possibilities for the production and exchange of heat between its surfaces. There are three types of heat load at very low temperature that might take place in a cryostat: (1) *Solid conduction* is a type of heat transfer in which there exists a temperature gradient between the two solid surfaces in the supporting systems. (2) *Residual gas conduction* is a type of heat transfer that occurs between a surface and a moving liquid when they are at different temperatures of non–perfect vacuum insulation and (3) *Thermal radiation* is a mode of the heat transfer between two surfaces at different temperatures in the absence of media, which means it can propagate in vacuum too [2]. In fact, thermal radiation is the most important and major part of the total produced heat load in the cryostats. All of these heat loads can be minimized in various ways by following appropriate procedures. Solid conduction can be minimized by making a suitable and appropriate choice of the material. Residual gas conduction can be minimized by creating a perfect vacuum in between the walls of the cryostat. Thermal radiation can be minimized by placing the radiation shields with spacers in between the cold and hot surfaces of a cryostat. Therefore, understanding of the thermal radiation reduction requires appropriate consideration of the heat transfer between these two surfaces [22]. The present work focuses on the reduction of thermal radiation heat load.

In the minimization of thermal radiation, an opaque body would be a good approximation in designing the cryostat structure. This is because an opaque body has zero–transmissivity to the electromagnetic radiation incident over it. It follows that all the received energy is either absorbed or reflected from the surface of such a body. However, this approximation fails in the presence of an orifice in the thermal shield. Such hole or crack leads shining of radiation through them and finally, these radiations get absorbed by the internal surfaces via multiple reflections. Then the body will behave like a black body with full absorptivity. Therefore, such gaps, holes and, slots must be avoided by taking great care during the designing of thermal shields, which may be pernicious to the thermal performance of cryostats [2]. If such gaps are unavoidable (when thermal contraction compensation gaps need to be surely introduced), then MLI blankets (reflective layer + spacer) can

be used to avoid shining light through them. However, in ultra-high vacuum applications (where MLI blankets can't be used) such gaps need to be surrounded by the traps of high-absorptivity and high-reflectivity materials (by making special coatings) to absorb and reflect the light incident on the wall of thermal shield and reduce the multi-path reflection on the inside surface.

This problem can be well understood by considering the radiation exchange between two surfaces. The heat exchange between the real surfaces of two bodies (with area  $A_1$  and  $A_2$  which are kept at temperatures  $T_1$  and  $T_2$  ( $T_1 > T_2$ ), respectively) greatly depends on their emissivity ( $\varepsilon$ ) which varies with the temperature and defines as the fraction of the emitted radiation  $E(T)$  with respect to that of a black body  $E_b(T)$  [2]

$$q_{1-2} = \varepsilon \sigma (T_1^4 - T_2^4) A_2 F_{21} \quad \text{where} \quad \varepsilon = \left[ \frac{E(T)}{E_b(T)} \right] \leq 1. \quad (2.1)$$

Here  $\sigma$  is the Stefan-Boltzmann's constant ( $5.675 \times 10^{-8} \text{ Wm}^{-2}\text{K}^{-4}$ ) and  $F_{21}$  is the geometrical view factor [23, 24], defined as the fraction of the total radiation leaving from the first body, which is intercepted and absorbed by the second body (it depends upon the relative orientation of the two surfaces). It follows the reciprocity rule such that  $A_1 F_{12} = A_2 F_{21}$  [25]. In case of metals at cryogenic temperatures, the  $\varepsilon$  reduces  $\sim \propto T$ . This leads to the enhancement in the low-emissivity properties of cryogenic cooled thermal shields in cryostats.

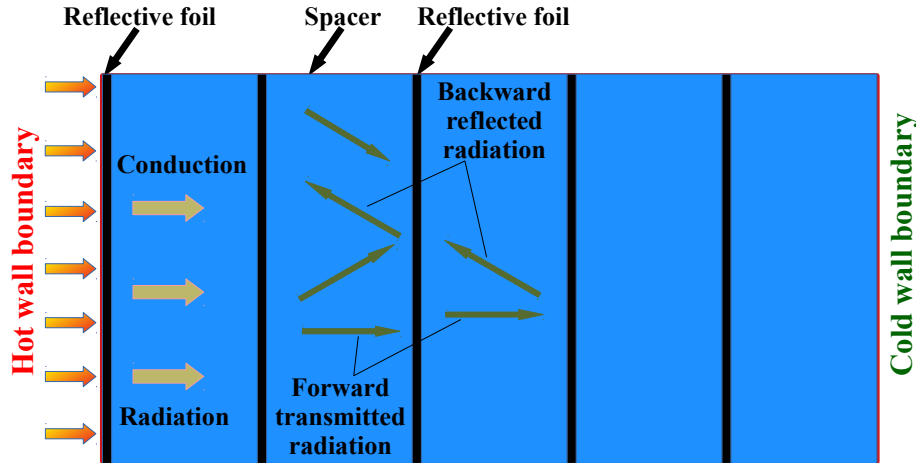


**Figure 2.** Basic functioning of MLI technique. Heat load tremendously decreases as the heat radiation move on to the consecutive reflective layers.

It is the geometries which play a crucial role in the designing of cryostats. Generally, the heat transfer by radiation between two enclosed surfaces (from one which is at  $T_1$  with  $\varepsilon_1$  and surface area  $A_1$ , to another at  $T_2$  with  $\varepsilon_2$  and  $A_2$ , such that  $T_1 > T_2$ ) can be expressed as [8]

$$q_{1-2} = \frac{\sigma (T_1^4 - T_2^4)}{\left( \frac{1-\varepsilon_1}{\varepsilon_1 A_1} + \frac{1}{A_2 F_{21}} + \frac{1-\varepsilon_2}{\varepsilon_2 A_2} \right)}. \quad (2.2)$$

The present work focuses on the comparative study of radiation heat load calculation in the cylindrical and spherical designs. The heat exchange between two enclosed cylinders with  $A_1$  and  $A_2$

being the outer and inner surfaces respectively, and kept at temperatures  $T_1 > T_2$ ,  $F_{21} = 1$  (because surface  $A_2$  is completely surrounded by the surface  $A_1$  [26] as shown in figure 3(c)), from energy balance and use of Eq. (2.1) [27, 28]

$$q_{1-2} = \frac{\sigma A_2 (T_1^4 - T_2^4)}{\frac{1}{\varepsilon_2} + \frac{1-\varepsilon_1}{\varepsilon_1} \left( \frac{A_2}{A_1} \right)}. \quad (2.3)$$

The heat exchange between two concentric spheres, with  $A_1$  and  $A_2$  being the outer and inner surfaces respectively, and kept at temperatures  $T_1 > T_2$ , such that the heat transfer takes place from out-to-inside, follows the same expression as in Eq. (2.3) [29]. The heat exchange for parallel flat plates of area  $A = A_1 = A_2$ ,  $F_{21} = 1$ , when  $T_1 > T_2$ , is given by

$$q_{1-2} = \frac{\sigma A (T_1^4 - T_2^4)}{\left( \frac{1}{\varepsilon_1} + \frac{1}{\varepsilon_2} - 1 \right)}, \text{ and for same material } (\varepsilon_1 = \varepsilon_2 = \varepsilon) \equiv \frac{\sigma A (T_1^4 - T_2^4)}{\left( \frac{2}{\varepsilon} - 1 \right)}. \quad (2.4)$$

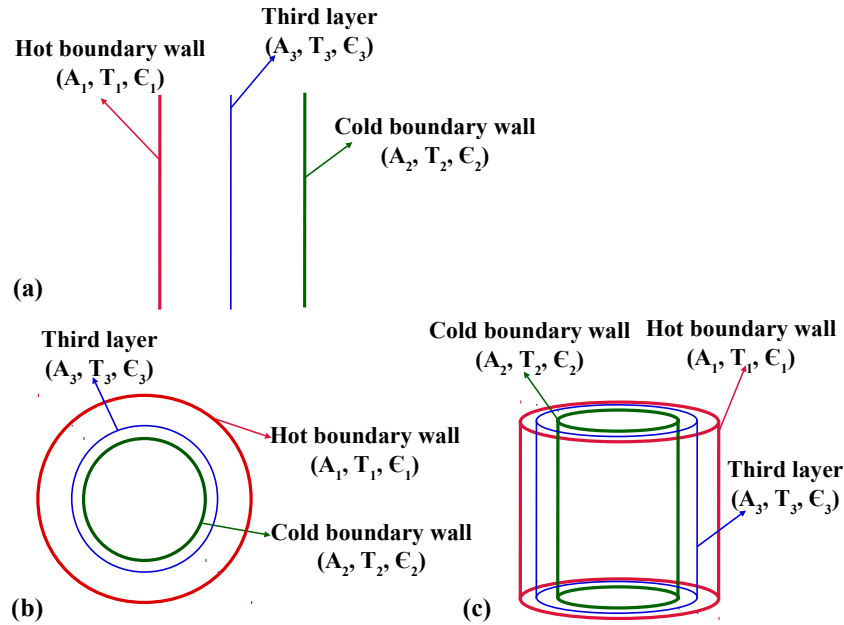


**Figure 3.** Schematic diagrams of (a) parallel plate (b) spherical, and (c) cylindrical geometries of a cryostat with the insertion of a third intermediate layer.

It is obvious from Eqns. (2.2), (2.3), and (2.4) that the heat transfer can be minimized by using the low emissivity materials. As emissivity depends on the material as well as surface finishing and cleanliness, clean and well-polished metallic surfaces have low emissivity, whereas non-metallic surfaces have higher emissivity. Thus, thermal shields (walls) in the cryostat are normally made up of properly polished metallic surfaces (Copper or Aluminium) [2]. Copper is the most promising material for this purpose because: (1) It has less emissivity as compare to Aluminium, after proper mechanical polishing [2]. (2) Rare to brittle even at very low temperatures [30]. (3) It can be stored in underground storage and quickly moved to the processing sites [31]. (4) The amount of cryogenic liquid used to cool 1 kg of Copper is less in comparison with other cryostat materials [30].

(5) Irradiation of Copper will produce  $^{60}\text{Co}$  whose lifetime is less as compared to those which are produced by other materials [30].

Furthermore, if one introduces a third intermediate plate between the two plates, whose temperature is the average of the temperatures  $\left(T_3 = \frac{T_1 + T_2}{2}\right)$  of the two plates, with  $\varepsilon_{31}$  and  $\varepsilon_{32}$  being its corresponding temperature-dependent emissivities, the general form of the heat exchange through the walls can be expressed as

$$q_{1-2} = \frac{\sigma(T_1^4 - T_2^4)}{\frac{1-\varepsilon_2}{\varepsilon_2 A_2} + \frac{1}{A_2 F_{23}} + \frac{1-\varepsilon_{32}}{\varepsilon_{32} A_3} + \frac{1-\varepsilon_{31}}{\varepsilon_{31} A_1} + \frac{1}{A_3 F_{31}} + \frac{1-\varepsilon_{31}}{\varepsilon_{31} A_3}} . \quad (2.5)$$

In case of parallel plates ( $A_1 = A_2 = A_3 = A$ ),  $F_{23} = F_{31} = 1$  as schematized in figure 3(a), this heat exchange would be reduced by a factor of two [2] by the insertion of the same material ( $\varepsilon_{31} = \varepsilon_{32} = \varepsilon_3 = \varepsilon$ )

$$q_{1-2} = \frac{\sigma A(T_1^4 - T_2^4)}{2\left(\frac{2}{\varepsilon} - 1\right)} . \quad (2.6)$$

In the case of spherical as well as cylindrical geometries with  $A_1 > A_3 > A_2$ , whose schematic diagrams are shown in figure 3(b) and (c), the general form of heat exchange (Eq. (2.2)) would take place the following form

$$q_{1-2} = \frac{\sigma A_2(T_1^4 - T_2^4)}{\frac{1}{\varepsilon_2} + \left(\frac{1}{\varepsilon_1} - 1\right) \frac{A_2}{A_1} + 2\left(\frac{1}{\varepsilon_3} - 1\right) \frac{A_2}{A_3} + \frac{A_2}{A_3}} . \quad (2.7)$$

Thus, in the case of spherical and cylindrical geometries, the heat load is also reduced nearly by a factor of two due to the insertion of a third intermediate layer as in the case of a parallel plate geometry.

This is a valuable hint about how the radiation heat load in a cryostat can be decreased by inserting a new third layer (or more layers) in between the hot and cold walls of the cryostat. This leads the people to proceed towards the MLI technique. In the MLI technique, the radiation heat from the outer space strikes on its first reflective layer. A part of heat radiation is reflected from this reflective layer and remaining radiation energy heats the first layer of the spacer. With the increment in the temperature of this spacer layer, solid conduction, gas conduction and radiation start taking place via the spacer material to the next reflective layer. It follows that the temperature of the second reflective layer will further increase. The second reflective layer reflects a part of the incident radiation to the first spacer layer and transfers the remaining energy to the second spacer layer [5]. This process continues up to the last bottom layer and results in an immense reduction in heat load. The basic functioning of the MLI is represented in figure 2.

### 3 Optimization of the layer density in MLI technique

Selecting a suitable number of MLI layers is quite crucial and affects its efficiency at a significant level. It depends on the thickness as well as material of reflective layers employed, the thickness of coated Aluminium, type of spacers, thickness of blanket, residual gas pressure, etc. Therefore, it doesn't allow for introducing as many layers as can fit in the available space. This is because of

using more radiation shields within a fixed available space might introduce other possible ways for the heat exchange such as: (1) Radiation between the shields, because the thickness of spacers is reduced, (2) Heat exchange due to solid conduction between radiation shields through the spacers is introduced, and (3) Gas conduction due to the presence of gas molecules between the radiation shields and spacers. Therefore in every MLI system, an optimum layer density (number of layers/cm) is defined where the heat transfer is minimum. A schematic diagram of the MLI system along with the heat exchange via heat radiation, solid conduction, and gas conduction between two consecutive reflective layers is shown in figure 2.

Large number of radiation shields within a fixed available space are responsible for the increment in the thermal contact. Consequently, solid conduction increases within these radiation shields. Furthermore, a large number of radiation shield means increase of material and assembly costs in the experiment. It follows that the layer density must be optimized [18, 32]. This optimization can be performed by varying the distance between layers and adjusting the number of layers within a fixed thickness of the insulation blanket. After the optimization of layer density, one needs to optimize the thickness of the blanket having the constant layer density. This is because the layer density is the same for all thicknesses if all the conditions and materials remain the same.

There are two important analytical approaches available to optimize the layer density: (1) Modification of Lockheed equation, and (2) Theoretical calculation developed for Layer-by-Layer approach by McIntosh. In the Modified Lockheed equation [33], the original Lockheed equation is modified by accounting the conductivity term for spacers in the solid conduction term by McIntosh. This approach accounted for all three modes of heat exchange [32]:

$$q_{\text{total}} = q(\text{radiation}) + q(\text{solid conduction}) + q(\text{gas conduction}) . \quad (3.1)$$

The generalized form of the Modified Lockheed equation provides an empirical form of the heat flux such as [7]:

$$q_{\text{total}} = \frac{C_R \varepsilon (T_h^{4.67} - T_c^{4.67})}{N} + \frac{C_S \bar{N}^{2.63} (T_h - T_c)(T_h + T_c)}{2(N + 1)} + \frac{C_G P (T_h^{0.52} - T_c^{0.52})}{N} , \quad (3.2)$$

where  $\bar{N}$  is the layer density and  $N$  represents the number of layers. The term  $C_S$  is the solid conduction coefficient and it is a function of spacer's material. Symbol  $C_R$  is the radiation coefficient and it is a function of reflector's material. The  $C_G$  is the gas conduction coefficient and it is a function of radiation gas pressure between the layers. Here  $T_h$  is the outer (hot) layer temperature (in K),  $T_c$  is the inner (cold) layer temperature (in K), and  $P$  symbolizes the residual gas pressure. The Lockheed Equations are essentially based on the data from MLI systems (mainly composed of double-Aluminized Mylar radiation shields with Silk-net spacers), which are tested using a flat plate but not the case of cylindrical calorimeter [34]. The Modified Lockheed equation can not be used for Layer-by-Layer approach because of the presence of  $(N + 1)^{\text{th}}$  term in the denominator of Eq. (3.2).

One another important approach is the physics-based expression developed by McIntosh for the theoretical calculation of an MLI system performance [35]. This approach also accounts for all the above mentioned (Eq. (3.1)) three modes of the heat exchange like the Lockheed Equations. All of these modes of heat exchange vary from layer to layer but, the total heat flux remains constant



across the whole MLI-blanket. It follows that this approach applies to a complete MLI system rather than a Layer-by-Layer approach. In McIntosh approach, the heat radiation exchange term comprises of [32]:

$$q_{\text{radiation}} = \frac{\sigma(T_h^4 - T_c^4)}{\left(\frac{1}{\varepsilon_h} + \frac{1}{\varepsilon_c} - 1\right)}, \quad (3.3)$$

where  $\varepsilon_h$  and  $\varepsilon_c$  are the emissivities of the hot and cold surfaces, respectively. The heat exchange through the gas conduction term consists of [36]:

$$q_{\text{gas conduction}} = C_G P \alpha (T_h - T_c), \quad (3.4)$$

where  $C_G = K_G / P \alpha$ , in which  $K_G$  is the gas conduction (in  $\text{Wm}^{-2}\text{K}^{-1}$ ),  $P$  is the gas pressure (in pa),  $C_G = [(\gamma + 1)/(\gamma - 1)][R/8\pi MT]^{\frac{1}{2}}$  and its value is 1.1666 for the air and 2.0998 for the Helium,  $\alpha$  is the accommodation coefficient,  $\gamma = C_p/C_v$ ,  $R$  is the gas constant ( $8.314 \text{ kJ}\cdot\text{mol}^{-1}\text{K}^{-1}$ ),  $M$  is the molecular weight of gas (in  $\text{kg}\cdot\text{mol}^{-1}$ ) and  $T$  is the temperature of vacuum gauge (usually  $\sim 300 \text{ K}$ ) [5]. Lastly, the heat exchange via the solid conduction term represents:

$$q_{\text{solid conduction}} = K_S (T_h - T_c), \quad (3.5)$$

where  $K_S = C_S f k / \Delta x$ , in which  $C_S$  is an empirical constant,  $f$  is the relative density of the separator compared to solid material,  $k$  is the separator material conductivity (in  $\text{Wm}^{-1}\text{K}^{-1}$ ) and  $\Delta x$  ( $\equiv (d_o - d_i)$ ) difference between the outer ( $d_o$ ) and inner ( $d_i$ ) diameter of the specimen) is the actual thickness separator between reflectors (in meter) [4]. Therefore the total heat transfer in McIntosh's approach comes out to be the sum of Eqns. (3.3), (3.4) and (3.5):

$$q_{\text{total}} = \frac{\sigma(T_h^4 - T_c^4)}{\left(\frac{1}{\varepsilon_h} + \frac{1}{\varepsilon_c} - 1\right)} + C_S f k \left(\frac{T_h - T_c}{\Delta x}\right) + C_G P \alpha (T_h - T_c). \quad (3.6)$$

It is obvious from the Modified Lockheed equation (3.2) and McIntosh equation (3.6) that the optimization of the layer density ( $\bar{N}$ ) requires the selection and declaration of coefficients  $C_S$ ,  $C_G$  and  $C_R$ , whose values depend on the type of materials used. Reflector material is responsible for the radiation between shields and radiant heat transfer is proportional to the  $\varepsilon$  of shields. It follows that low  $\varepsilon$  materials must be used to form reflectors [37]. There are two most frequent applicable reflectors: (1) Thin Aluminium-foil, and (2) Polymeric film composed of polyester (Mylar) coated with Aluminium on both sides called Double-Aluminized-Mylar; or composed by Polyimide (Kapton) [13, 37].

The spacer material is responsible for the solid conduction between reflector sheets through spacers. Furthermore, the heat transfer through spacers is proportional to the thermal conductivity of the material. Therefore, low conductivity materials like Silk-net, Polyester-net, Fiberglass cloth, Fiberglass mats, Paper, Rayon fiber paper, etc. are used to form spacers [7].

In case of imperfect vacuum insulation, the residual gaseous conduction can develop a nontrivial contribution to the total heat transfer. It depends on the level of vacuum, the type and amount of residual gas, geometry, and temperatures involved [38]. Generally, the level of vacuum between layers is unknown and can have considerable effects on the thermal performance of the MLI system. It should be noted that the residual gas conduction is proportional to the pressure and temperature

difference ( $T_h - T_c$ ) between walls [2]. Thus it can be minimized by lowering the pressure of the gas ( $P \lesssim 10^{-4}$  torr). To account for and explain all the thermal performance results of MLI system, it requires an understanding of all the available information from the heating, purging, evacuation, and vacuum monitoring steps [7].

Although one can use more radiation shields to reduce the radiation, the solid conduction between radiation shields increases through the spacers due to the decreased space between two radiation shields and the thickness of spacers. It follows that there must be a balance point between the radiation and solid conduction heat load, which is also called as optimum layer density. In the following section, we will elaborate the optimization of layer density for achieving the minimum heat transfer.

## 4 Results and discussion

A stable temperature of the cryogenic liquid can be achieved by reducing the heat load coming from the outer wall of the cryostat. Numerous approaches have been tested and are being utilized to reduce the heat load. An optimum level of vacuum is required between the two walls of the cryostat to reduce the gaseous conduction heat load. Furthermore, in order to reduce the loss of cryogenic liquid due to evaporation, the silver coating has also been done at the inner surface of the outer wall and the outer surface of the inner wall, but still, heat load persists at significant level [13]. The present work will not go into the detail of the optimization of the vacuum level between the walls of the cryostat and the choice of suitable metallic coatings over them. This work is focused on the optimization of the MLI technique for the reduction of thermal radiation heat load to the cryogenic liquids.

### 4.1 MLI testing material

The current work assumes that the radiation shields and spacers in the MLI technique are placed perpendicular to the direction of the heat flow. These spacers are placed to avoid the thermal contact between the radiation shields because this causes the production of conductive heat load. In the testing of cryostat's thermal performance, the  $\varepsilon$  of the outer surface is chosen to be 0.043 for Aluminized radiation shields, optimum vacuum pressure  $P = 10^{-4}$  torr, residual gas is Nitrogen, and the cold and hot boundary temperatures are approximately 77 K for LN<sub>2</sub> and 300 K for water, respectively. This level of vacuum is required to minimize the conductive heat load produced by the presence of residual Nitrogen gas in between the walls of the cryostat. Furthermore, this partial conduction may also cause the condensation of moisture around the outside of the walls, which may further produce undesirable heat load on the cryogenic liquid [39].

The present analysis follows the robust Modified Lockheed equation (3.2) to evaluate the production of heat load in the MLI technique. The coefficients  $C_R$ ,  $C_G$ , and  $C_S$  used in this expression are material dependent. We have selected: (1) Unperforated double Aluminized Mylar sheet (DAM) with Silk-net, (2) Perforated DAM with Glass-tissue, and (3) Perforated DAM with Dacron materials as reflecting shields as well as spacers in the MLI technique. The values of coefficients  $C_R$ ,  $C_G$ , and  $C_S$  for these selected materials are listed in table 1.

The "solid conduction" term in the empirical expression (3.2) would be modified for the Dacron spacer material. It has been done because in the original Lockheed equation the spacer material used

**Table 1.** Selected reflective layer as well as spacer materials for the MLI technique with their respective coefficients.

Materials	Coefficients		
	$C_R$	$C_S$	$C_G$
Unperforated DAM with Silk-net [7]	$5.39 \times 10^{-10}$	$8.95 \times 10^{-8}$	$1.46 \times 10^{-4}$
Perforated DAM with Glass-tissue [32]	$7.07 \times 10^{-10}$	$7.30 \times 10^{-8}$	$1.46 \times 10^{-4}$
Perforated DAM with Dacron [32]	$4.94 \times 10^{-10}$	Shown in (4.1)	$1.46 \times 10^{-4}$

was Glass-tissue with different sizes of shield's perforation, whereas during testing the spacer used was Dacron material with dissimilar sizes of shield's perforation. It follows that the term containing "solid conduction" in (3.2) got modified for the Dacron material [32]. After incorporating this modification, the total heat flux expression for the Dacron becomes

$$q_{\text{total}} = \left( \frac{2.4 \times 10^{-4} (0.017 + 7 \times 10^{-6} (800 - T) + 0.0228 \ln(T)) \bar{N}^{2.63} (T_h - T_c)}{N} \right) + \left( \frac{C_R \varepsilon (T_h^{4.67} - T_c^{4.67})}{N} \right) + \left( \frac{C_G P (T_h^{0.52} - T_c^{0.52})}{N} \right), \quad (4.1)$$

where  $T$  is the average temperature  $\left(T = \frac{T_h + T_c}{2}\right)$  of the hot and cold boundaries. It is obvious from Eq. (4.1) that the term containing solid conduction segment is modified for the Dacron [32]. We will proceed with these important and necessary ingredients towards the parameter analysis.

## 4.2 Analysis of the key parameters in MLI technique

Apart from the selection of suitable radiation shield as well as spacer materials, the Layer density, number of layers, and thickness of insulating blanket, are the key parameters in getting excellent MLI with potential performance in reducing the thermal radiation heat load. In the present work, we have calculated the effect of layer density and the number of layers on the heat load and evaluated optimal layer density and favorable thickness of insulating blanket for these selected materials in the MLI technique.

### 4.2.1 Enhancement in layer density and its effect on the heat load

Radiation shields are generally coated with highly reflecting metals (Aluminium or Gold), to reflect the thermal radiation for reducing the radiation heat load. It follows that there may be a chance of conduction between them and may lead to the enhancement in the heat load. Thus, insulating spacers are used in between the radiation shields to solve this issue. Although the installation of insulating spacers causes the decrement in heat load, it doesn't reduce to a significant level. Therefore, more and more radiation shields with insulating spacers can be used to reduce the heat load. However, with the increment in  $\bar{N}$ , the heat load starts increasing due to the reduction of space between the radiation shields and thus solid conduction between the shields increases through the

spacers [2]. This increment in the heat load with  $\bar{N}$  for a fixed number of layers ( $N = 40$  is chosen as the reference for explanation), is shown in figure 4.

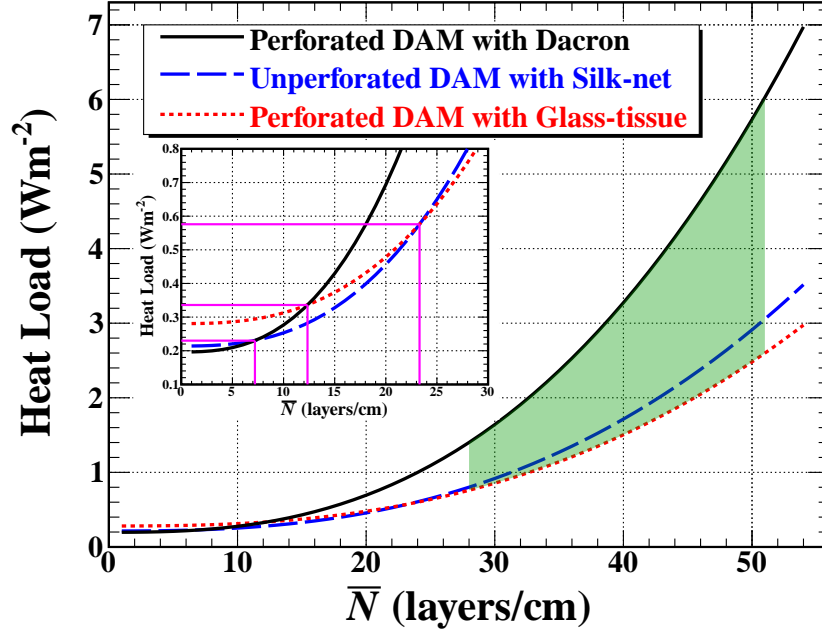


**Figure 4.** Variation in the heat load with the increment in  $\bar{N}$  for a constant number of layers ( $N = 40$ ). The effect of smaller  $\bar{N}$  choice on the heat load and the comparative material's behavior is shown in the inset.

It is obvious from figure 4 that the heat load increases with  $\bar{N}$  for all the three selected materials. In the light of Eq. (4.1) and coefficients of table 1, this increment in the heat load is quite larger for the Dacron in comparison to the Glass-tissue and Silk-net material at higher  $\bar{N}$ . However, below  $\bar{N} \sim 10$  the Dacron material leads to the minimum heat load among the three selected materials. It is also noteworthy in the inset of figure 4 that the perforated DAM with Glass-tissue and unperforated DAM with Silk-net for  $\bar{N} = 23.3$  produces equivalent heat load of  $0.58 \text{ Wm}^{-2}$ . Similarly, perforated DAM with Dacron and perforated DAM with Glass-tissue at  $\bar{N} = 12.3$  leads to the concordant heat load of  $0.34 \text{ Wm}^{-2}$ . Furthermore, perforated DAM with Dacron and unperforated DAM with Silk-net produces comparable heat load of  $0.23 \text{ Wm}^{-2}$  at  $\bar{N} = 7.2$ .

**Table 2.** Enhancement in the heat load with the increment in  $\bar{N}$  (from 28 to 51 layers/cm  $\equiv 82\%$ ) for the chosen reflective layer and spacer materials.

Reflective layer	Spacer material	Increment in $\bar{N}$ (%)	Enhancement in heat load (%)
Unperforated DAM	Silk-net	82	282
Perforated DAM	Glass-tissue		242
Perforated DAM	Dacron		330

The effect of enhancement in the layer density from  $\bar{N} = 28$  to 51 layers/cm ( $\equiv 82\%$  increment,

as a reference) on the heat load for the chosen materials is summarized in table 2. It is obvious from the shaded region of figure 4 that this increment in  $\bar{N}$  leads to severe enhancement in the heat load. This enhancement is even more profound for the perforated DAM with Dacron material in comparison to the unperforated DAM with Silk-net and perforated DAM with Glass-tissue. This drastic enhancement in the heat load marks that the value of  $\bar{N}$  can not be increased beyond a limit and must need to be optimized for different materials.

#### 4.2.2 Selection of optimal layer density

The optimization of  $\bar{N}$  has a great impact on achieving the better thermal performance of the MLI technique. The value of  $\bar{N}$  varies for different materials [29]. Radiation shields and spacers are used to reduce the radiation heat load. Consequently, this heat load reduces however, to minimize it significantly one may increase the number of radiation shields. A huge increment in the number of radiation shields (and thus  $\bar{N}$ ) lead the probable enhancement in the thermal contact between the radiation shields because of the decrement in spacer thickness as well as the space between radiation shields. This results in an increment in the solid conduction between the radiation shields through the spacers. Whereas, according to Eq. (3.2), the radiation heat load remains invariant for a constant value of  $N$ . It follows that there must be an equilibrium between the radiation and conduction heat loads. This equilibrium point would represent the optimal  $\bar{N}$  where the total heat load is minimum for that material [2, 18].

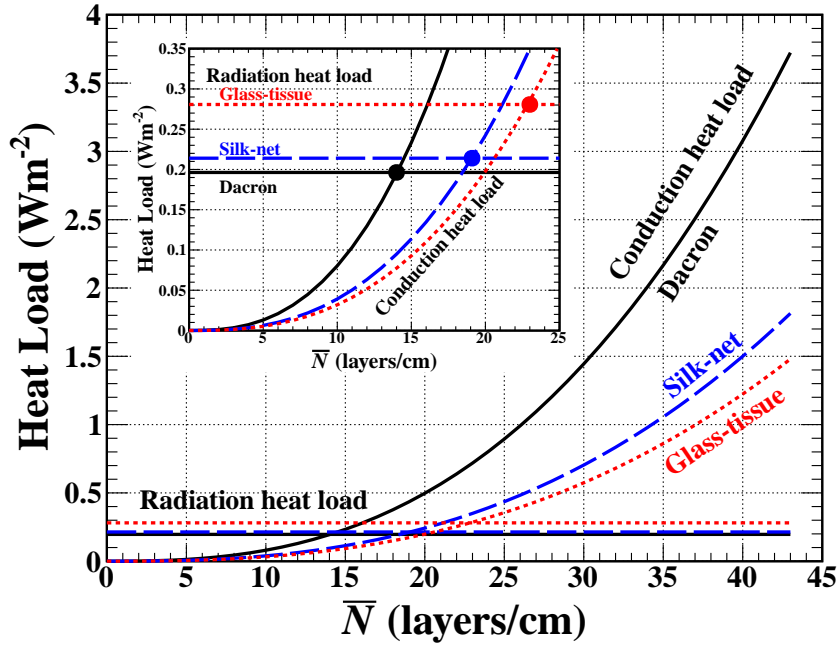


**Figure 5.** Variation in the heat load with  $\bar{N}$  for the chosen unperforated DAM with Silk-net, perforated DAM with Glass-tissue and perforated DAM with Dacron materials in the MLI technique. The intersecting contours (as shown in the inset) of radiation and conduction heat load represents the optimum value of  $\bar{N}$  for reference value of  $N = 40$ .

We have calculated the optimal  $\bar{N}$  for the selected perforated DAM with Glass-tissue, perforated

DAM with Dacron, as well as unperforated DAM with the Silk–net radiation shield and spacer materials for a reference  $N = 40$ . At this reference value of  $N$ , the variation of radiation and conduction heat load with  $\bar{N}$  is displayed in figure 5. Although the value of radiation heat load varies with the choice of material, remain constant for a selected constant value of  $N$  and shown by the horizontal contours for the selected materials. The equilibrium between the radiation and conduction heat load is zoomed and shown in the inset of figure 5. The intersection points (represented by solid dots) in the variation of conduction and radiation heat load with  $\bar{N}$  are the optimum values of  $\bar{N}$  for the respective materials. The optimum value of  $\bar{N}$  for a reference value  $N = 40$  is summarized in table 3 for the selected materials. If all the above mentioned criterion remains intact, the MLI insulating blanket's thicknesses would be the same for a given  $\bar{N}$ . It follows that the thickness of the insulating blanket needs to be optimized. As a consequence of the optimization in  $\bar{N}$ , the optimal thickness of the insulating blankets are also evaluated. These values are listed in the last column of table 3.

**Table 3.** Optimal values of  $\bar{N}$  and the thickness of insulating blanket for the selected unperforated DAM with Silk–net, perforated DAM with Glass–tissue and perforated DAM with Dacron materials for a reference value  $N = 40$ .

Reflective layer	Spacer material	Reference $N$	$\bar{N}$ (layers/cm)	Blanket's thickness (mm)
Unperforated DAM	Silk–net	40	19.0	21.1
Perforated DAM	Glass–tissue		22.7	17.6
Perforated DAM	Dacron		14.0	28.6

The outcome of table 3 exhibits that the perforated DAM with Glass–tissue can accommodate larger  $N$  within a fixed space between the cold and hot boundaries of cryostat in comparison to the unperforated DAM with Silk–net and perforated with DAM Dacron. Therefore, perforated DAM with Glass–tissue would be a better choice with optimal  $\bar{N}$  of 22.7 layers/cm, and optimal thickness 17.6 mm of blanket for a constant  $N = 40$  in making radiation shield and spacer for MLI technique. However, instead of a constant  $N$ , the effect of variable  $N$  on heat load needs to be considered before coming to the inference in the selection of material for MLI technique.

#### 4.2.3 Effects of increment in the number of layers over the heat load

After the evaluation of optimum values of  $\bar{N}$  (via variation between heat load and  $\bar{N}$ ), it becomes realistic to further quantify the effect of increment in  $N$  over the heat load. One has to increase the thickness of the MLI system for making increments in the value of  $N$  at the optimum and constant value of  $\bar{N}$ . This would result in a further decrement in the heat load because of the reduction in the thermal contact between the radiation shields.

Knowing the optimal values of  $\bar{N}$ , we have further investigated the effect of increment in the  $N$  at the constant values of  $\bar{N}$  for the selected materials. A variation of the heat load with  $N$  at constant  $\bar{N}$  is shown in figure 6, which exhibits an expected decrement in the heat load with  $N$ . In order to get the inference about the performance of the material, we have evaluated the decrement in heat

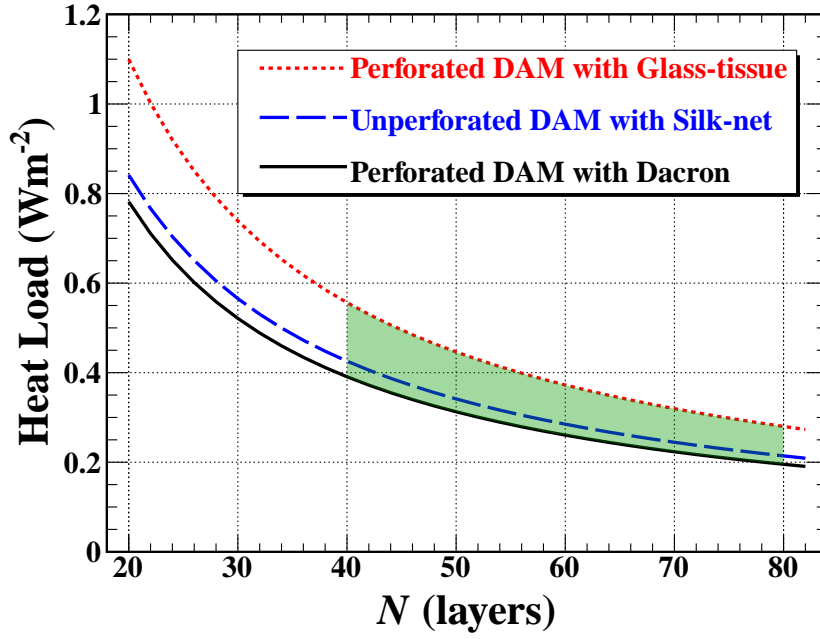


**Figure 6.** Effect of increment in the values of  $N$  over the heat load at the calculated optimum values of  $\bar{N}$  for the chosen materials. As a reference, the effect of an increment in  $N$  from 40 to 80 is shown by the shaded region.

**Table 4.** The expected decrement in the heat load with enhancement in the value of  $N$  at the constant and optimum values of  $\bar{N}$  for the chosen materials in MLI technique.

Reflective layer	Spacer material	Increment in $N$	Decrement in heat load (%)
Unperforated DAM	Silk-net	40 – 80	50.0
Perforated DAM	Glass-tissue		50.0
Perforated DAM	Dacron		50.0

load with an increment of 100% in  $N$  from 40 to 80 as shown by the shaded region in figure 6 and their outcomes are summarized in table 4 for the chosen materials.

It is obvious from table 4 and figure 6 that an increment in  $N$  by 100% (at the constant values of  $\bar{N}$  taken from table 3) causes for 50% decrement in heat load. As this decrement in heat load is evaluated at the respective optimum values of  $\bar{N}$ , for the selected materials, the decrement in heat load is exactly the same and material independent.

### 4.3 Preference in the geometry of the cryostat

Cryostats are being used with different perspectives in different experiments. They need to accommodate the cryogenic liquid along with the shielding around the detector, detectors immersed in the cryogenic liquid, and only cryogenic liquid, which also works as the detector, etc. Cylinders, parallel flat plates, and spheres with two enclosed envelopes are of particular interest in the cryostat design.

Apart from taking care of several aspects like the choice of material, selection of  $N$ , optimization of  $\bar{N}$ , the thickness of insulating blankets, appropriate geometry, the problem of buckling, etc., there is one common requirement in such cryostats is that, they all are intended to minimize their heat load.

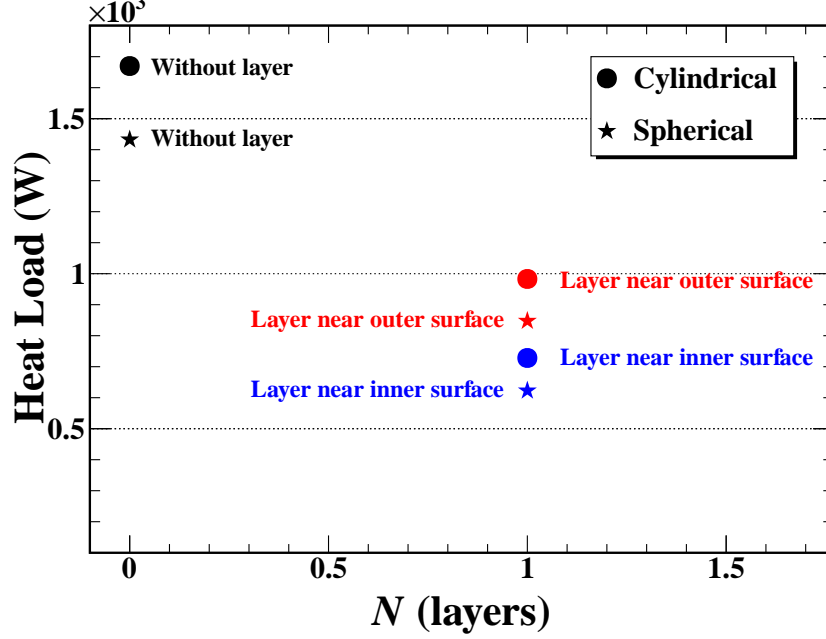


**Figure 7.** Comparison of the heat load production before and after insertion of one MLI layer near inner as well as outer surfaces in the spherical and cylindrical geometries of the cryostat.

The radiation exchange between two surfaces depends on their geometry, which can be well understood by the geometrical view factor [23, 24]. Therefore the geometry of a cryostat would need to be better designed under proper consideration of the total heat load. It follows that the analysis of all the key parameters discussed above in section 4.2 would have a significant impact on the selection of appropriate geometry for the cryostat in an experiment.

There are spherical, cylindrical and conical geometries of a cryostat, which are very common in experiments. The present work is focused on the comparison of cylindrical and spherical cryostats (with exactly the same volume) in the minimization of heat load. We have considered the dimensions of GERDA cryostat for comparison of geometries [15, 16]. A variation of heat load with a number of MLI layers for both of these geometries is shown in figure 7. It is explicit from figure 7 that the spherical cryostats are comparatively more suitable than the cylindrical ones in holding the cryogenic liquid for a longer time due to the less heat load. Therefore, spherical geometry is the most effective configuration because of having less heat load due to the least surface area to volume ratio. However, cylindrical cryostats are more preferably being used in several experiments because the fabrication of the cylindrical geometry is relatively easy and it is the most economical configuration in comparison to the spherical or conical geometries [40].

The effect of the MLI approach has a significant impact on reducing the heat load, which is obvious from figure 6. In the MLI technique, layering near the inner surface reduces heat load



nearly by a factor of two than layering close to the outer surface. This reduction in heat load by MLI technique is quite similar for both spherical as well as cylindrical geometries.

## 5 Summary and conclusion

MLI is an essential and important insulating technique used worldwide in the field of cryogenic as well as in the space industry. The efficient as well as long time storage, transfer of cryogenics, cooling of scientific instruments, and exploration of space demand a robust MLI technique in thermal insulation systems. It follows that a tremendous investigation is being performed since the last two decades in the field of MLI for a range of environments from high vacuum to no vacuum. A vigorous MLI system following a “thermo-economic” approach must need to consider the design of cryostat, appropriate radiation shield as well as spacer material, transmissivity of MLI, interstitial gas and its pressure, structural supports, and other mechanical obstacles to achieve the best MLI system.

The present work has analyzed the performance of perforated DAM with Dacron, unperforated DAM with Silk-net and perforated DAM with Glass-tissue as the radiation shield as well as spacer materials in MLI technique. This analysis follows the robust Modified Lockheed equation (3.2) to calculate the production of heat load in the MLI technique with these materials. In the present work, we have calculated the effect of layer density and number of layers on the heat load and evaluated optimal layer density and favorable thickness of insulating blanket for these selected materials in MLI technique.

It is observed that the increment in layer density causes the increment in heat load due to the reduction of space between the radiation shields and thus solid conduction between the shields increases through the spacers. This enhancement in heat load is significantly larger for the perforated DAM with Dacron and comparatively smaller for perforated DAM with Glass-tissue. With an increment in layer density from 28 to 51 layers/cm for a constant 40 insulating layers, the heat load increases by 330% in case of perforated DAM with Dacron, whereas this increment in the heat load is around 242% for perforated DAM with Glass-tissue. This huge enhancement in the heat load reveals the necessity for the optimization of layer density.

According to the Modified Lockheed equation (3.2), the radiation heat load remains constant whereas, the conduction heat load increases with layer density for a selected constant number of insulating layers. Therefore, there must be an equilibrium point between the radiation and conduction heat loads. The total heat load is minimum at this equilibrium point for that material and thus provides the optimal layer density. The optimal layer density for perforated DAM with Glass-tissue comes out to be 22.7 layers/cm (optimal blanket's thickness = 17.6 mm) which is the best among the three selected materials and the most conservative 14.0 layers/cm (optimal blanket's thickness = 28.6 mm) for the perforated DAM with Dacron. Furthermore, an increment of 100% in the number of layers at these optimal layer densities for the respective materials leads to 50% decrement in the heat load. Therefore, perforated DAM with Glass-tissue would be a better choice by optimal layer density and thickness of blanket in making radiation shield and spacer for getting the lowest heat load among the three chosen materials in the MLI system.

The inference of this analysis has a significant impact on the selection of appropriate geometry for the cryostat in an experiment. In the present, work we have compared the effect of MLI

technique on the heat load in cylindrical and spherical cryostats. It comes out that, in comparison to the cylindrical cryostat, the spherical cryostat leads to the less heat load and thus more suitable in holding the cryogenic liquid for a longer time. The MLI technique has a significant impact on reducing the heat load and a single layering near the inner surface of cryostat reduces heat load nearly by factor of two than the layering close to the outer surface.

## Acknowledgments

The author D. Singh gratefully acknowledges Council of Scientific and Industrial Research (CSIR-UGC), New Delhi, India, for the financial support in the form of CSIR (JRF/SRF) fellowship. The authors D. Singh, A. Pandey, and V. Singh are thankful to the Ministry of Human Resource Development (MHRD), New Delhi, India for the financial support through Scheme for Promotion of Academic and Research Collaboration (SPARC) project No. SPARC/2018–2019/P242/SL.

## References

- [1] Y. B. Cohen, *Low Temperature Materials and Mechanisms*, CRC Press Chapter **6** (2016) 109.
- [2] V. Parma, *Cryostat Design*, CERN Yellow Report **CERN-2014-005** (2013) 353 [arXiv:1501.07154].
- [3] J. Meseguer et al., *Spacecraft thermal control*, Cambridge: woodhead publishing limited Chapter **7** (2012) 111.
- [4] A. Hedayat et al., *Analytical modeling of variable density multilayer insulation for cryogenic storage*, *AIP Conference Proceedings* **613** (2002) 1557.
- [5] P. M. Suthesh et al., *Thermal performance of multilayer insulation: A review*, *OP Conf. Ser.: Mater. Sci. Eng.* **396** (2018) 012061.
- [6] J. E. Fesmire et al., *Robust Multilayer Insulation for Cryogenic Systems*, *AIP Conference Proceedings* **985** (2008) 1359.
- [7] J. E. Fesmire et al., *Cylindrical cryogenic calorimeter testing of six types of multilayer insulation systems*, *Cryogenics* **89** (2018) 58.
- [8] B. Baudouy, *Heat Transfer and Cooling Techniques at Low Temperature*, CERN Yellow Report **CERN-2014-005** (2015) 329 [arXiv:1501.07153].
- [9] EDELWEISS Collaboration, E. Armengaud et al., *Final results of the EDELWEISS-II WIMP search using a 4-kg array of cryogenic germanium detectors with interleaved electrodes*, *Phys. Lett. B* **702** (2011) 329.
- [10] EDELWEISS Collaboration, E. Armengaud et al., *Search for low-mass WIMPs with EDELWEISS-II heat-and-ionization detectors*, *Phys. Rev. D* **86** (2012) 051701(R).
- [11] CRESST collaboration, G. Angloher et al., *Results from 730 kg days of the CRESST-II Dark Matter search*, *Eur. Phys. J. C* **72** (2012) 1971.
- [12] A. Brown et al., *Extending the CRESST-II commissioning run limits to lower masses*, *Phys. Rev. D* **85** (2012) 021301(R).
- [13] EURECA Collaboration, G. Angloher et al., *EURECA Conceptual Design Report, Physics of the Dark Universe* **3** (2014) 41.
- [14] A. D’Addabbo et al., *The CUORE Cryostat*, *Journal of Low Temperature Physics* **193** (2018) 867.

- [15] GERDA Collaboration, I. Abt et al., *GERDA Technical Proposal 1* (2005) 25.
- [16] GERDA Collaboration, I. Abt et al., *GERDA Technical Proposal 2* (2006) 24.
- [17] LEGEND Collaboration, V. D'Andrea, *Neutrinoless Double Beta Decay Search with  $^{76}\text{Ge}$ : Status and Prospect with LEGEND* (2019) [arXiv:1905.06572].
- [18] W. L. Johnson, *Optimization of layer densities for multilayered insulation systems*, *AIP Conference Proceedings* **1218** (2010) 804.
- [19] W. D. Cornell et al., *Radiation shield supports in vacuum insulated containers*, *US Patent No. 2643022* (1947).
- [20] W. L. Johnson, *Thermal Coupon Testing of Load-Bearing Multilayer Insulation*, *AIP Conference Proceedings* **1573** (2014) 725.
- [21] S. D. Augustynowicz and J. E. Fesmire, *Cryogenic Insulation System for Soft Vacuum*, *Advances in Cryogenic Engineering*, Springer (2000) 1691.
- [22] J. G. Weisend II, *Cryostat Design: Case Studies, Principles and Engineering*, Springer (2016).
- [23] M. F. Modest, *Radiative Heat Transfer*, Academic Press, Third Edition (2013) 904.
- [24] [http://webserver.dmt.upm.es/isidoro/tc3/Radiation View factors.pdf](http://webserver.dmt.upm.es/isidoro/tc3/Radiation%20View%20factors.pdf)
- [25] F. P. Incropera et al., *Fundamentals of Heat and Mass Transfer*, 5th ed. (John Wiley & Sons, New York) (2002).
- [26] [http://www.mhtl.uwaterloo.ca/courses/syde381/lectures/summary/summary\\_ch15\\_S14\\_381.pdf](http://www.mhtl.uwaterloo.ca/courses/syde381/lectures/summary/summary_ch15_S14_381.pdf)
- [27] J. P. Elchert, *Cryogenic multilayer insulation theory and an analysis of seams under a variety of assumptions*, *Thermal and Fluids Analysis Workshop (TFAWS)*, August 20-24, 2018, Galveston, United States (2018).
- [28] V. Parma, *Cryostat Design*, *CERN Accelerator School: Superconductivity for Accelerators*, Erice, Italy, April 24-May 4 (2013).
- [29] <https://www.coursehero.com/file/44067079/AME60634-F13-lecture27pdf/>
- [30] G. K. White, *The thermal and electrical conductivity of copper at low temperatures*, *Austr. J. Phys.* **6** (1953) 397.
- [31] N. H. Balshaw, *Practical Cryogenics: An Introduction to Laboratory Cryogenics*, Oxford Instruments Superconductivity Limited (2001).
- [32] A. Hedayat et al., *Variable density multilayer insulation for cryogenic storage*, 36th AIAA/ASME/SAE/ASEE Joint Propulsion Conference and Exhibit (2000).
- [33] C. W. Keller et al., *Thermal Performance of Multi-Layer Insulations*, Final Report, Contract NAS3-14377, Lockheed Missiles & Space Company (1974).
- [34] G. R. Cunningham et al., *Thermal performance of multilayer insulations*, interim report LMSC-A903316/NASA CR-72605 Sunnyvale, CA: Lockheed Missile and Space Company (1971).
- [35] G. E. McIntosh, *Layer-by-layer MLI calculation using a separated mode equation*, *Advances in Cryogenic Engineering*, NY: Plenum Press **39B** (1993) 1683.
- [36] R. J. Corruccini, *Gaseous heat conduction at low pressures and temperatures*, *Vacuum* **7-8** (1959) 19.
- [37] J. R. Miller et al., *MLI Blanket Effective Emittance Variance and its Effect on Spacecraft Propellant Line Thermal Control*, 46th International Conference on Environmental Systems, Vienna, Austria **56** (2016).

- [38] J. R. Feller et al., *Dependence of multi-layer insulation thermal performance on interstitial gas pressure*, *AIP Conference Proceedings* **1434** (2012) 47.
- [39] M. N. Jirmanus, *Introduction to laboratory cryogenics*, Janis Research Company, Inc. (Willmington, Janis) (2009) 40.
- [40] G. B. Thapa, *Design of a Laboratory Nitrogen Liquefier cum Cryostat Based on Closed Cycle Refrigerator*, Master Thesis, National Institute of Technology Rourkela, India (2013).